TECHNICAL REPORT #6

Office of Naval Research
Contract Nonr-2121(22)

MAGNETO-ACOUSTIC EFFECTS IN TILTED MAGNETIC FIELDS†

Harold N. Spector*

Institute for the Study of Metals
and
Department of Physics

University of Chicago
Chicago, Illinois

June 1961

†Submitted in partial satisfaction of the requirements for the Ph.D. in Physics, University of Chicago

*Shell Oil Company Predoctoral Fellow, 1960-61

Magneto-Acoustic Effects in Tilted Magnetic Fields*†

Harold N. Spector**

Institute for the Study of Metals
and
Department of Physics
University of Chicago
Chicago, Illinois

Abstract

We have shown that the entire Fermi surface can be mapped by using geometic resonances in the sound attenuation in tilted magnetic fields and the drift velocity of the carriers along the magnetic field simultaneously determined. The general features of the phenomena considered do not prove dependent on the particular models used in our calculations.

In addition to the results specifically pertaining to tilted fields, we have found that when the assumptions of equal effective masses and relaxation times are dropped for a two band model of a semi-metal, the contribution of the two types of carriers to the ultrasonic absorption is additive. On examining the contribution to the absorption for a model of majority and minority carriers, we have found, also, that the minority carriers dominate the attenuation when they are in the region of geometric resonances.

---

* Submitted in partial satisfaction of the requirements for the degree of Ph.D. in Physics, University of Chicago.

† Supported in part by the National Science Foundation, and the the Office of Naval Research.

**Shell Oil Predoctoral Fellow, 1960-61.

I. Introduction

In the past few years, experiments have been performed on magneto-acoustic absorption in metals and semi-metals at low temperatures.[1-7] Several interesting phenomena have been observed which prove useful in determining the electronic structure of metals. In a transverse magnetic field, there are oscillations in the ultrasonic attenuation with magnetic field.[8-11] These oscillations occur when the cyclotron diameter of an extremal orbit is equal to an integral number of wave lengths. Also, in the high field limit, when the magnetic field is tilted from a direction perpendicular to the direction of propagation of the sound wave, there is an increase in the attenuation.[12] This increase occurs when the carriers drifting along the field with the maximum velocity remain in exact phase with the sound wave. The extremal dimensions of the Fermi surface can be obtained from the periods of the magneto-acoustic oscillations while the Fermi velocity can be determined from the critical angle of tilt at which the increase in attenuation begins.

The possibility of combining the tilt effect and the geometric resonance experiments to obtain information about the dimensions of non-extremal orbits on the Fermi surface now presents itself.[13] Through such an experiment, the whole Fermi surface could be mapped out.

In Section II we derive the expressions for the conductivity tensor that are appropriate in the region of geometric resonances for tilted fields. In Section III we treat the calculation of the ultrasonic attenuation for the case of the free electron gas in a uniform positive background discussed by Cohen, Harrison, and Harrison[8] as a model for a metal. In Section IV we do the same type of calculation for a two spherical band

model of a semi-metal discussed by Harrison.[14] We also examine the effect of relaxing his assumptions of equal effective masses and relaxation times for the two kinds of carriers. Section V is devoted to calculating the acoustic attenuation for a model of majority and minority carriers with a positive background. A discussion of the various phenomena which we have investigated theoretically and of their physical significance is given in Section VI.

II. Derivation of the Conductivity Tensor

Previous theoretical work has indicated that the geometric resonance[8] and the tilt effect[12] arise from the dependence of the components of the conductivity tensor on the magnetic field strength and the angle of tilt. We therefore begin by evaluating the components of the conductivity tensor in the region of geometric resonance for arbitrary angle between the direction of propagation and the magnetic field. The general expressions for the conductivity tensor in the presence of a magnetic field derived by Cohen, Harrison, and Harrison[8] using a model of a free electron gas are

$$\sigma_{xx} = \frac{3}{2}\frac{\sigma_0}{(q l \cos\nu)^2}\left\{ 2(1-i\omega\tau) - \sum_{n=-\infty}^{+\infty}\int_0^{\pi} d\theta \sin\theta \right.$$

$$\left. \frac{J_n^2(X\cos\nu\sin\theta)\left[1 + i(q l \sin\nu\cos\theta - \omega\tau)\right]^2}{1 + i(n\omega_c\tau - \omega\tau + q l \sin\nu\cos\theta)} \right\} \qquad \text{(II.1)}$$

$$\sigma_{yy} = \frac{3}{2}\sigma_0 \sum_{n=-\infty}^{+\infty}\int_0^{\pi} \frac{\sin^3\theta\left[J_n'(X\cos\nu\sin\theta)\right]^2 d\theta}{1 + i(n\omega_c\tau - \omega\tau + q l \sin\nu\cos\theta)}$$

$$\sigma_{zz} = \frac{3}{2}\sigma_0 \sum_{n=-\infty}^{+\infty}\int_0^{\pi} \frac{\cos^2\theta\sin\theta\, J_n^2(X\cos\nu\sin\theta)\, d\theta}{1 + i(n\omega_c\tau - \omega\tau + q l \sin\nu\cos\theta)}$$

$$\sigma_{xy} = -\sigma_{yx} = \frac{3}{4}\frac{\sigma_0}{q l \cos\nu}\sum_{n=-\infty}^{+\infty}\frac{d}{dX}\int_0^{\pi} d\theta \sin\theta\, J_n^2(X\cos\nu\sin\theta)$$

$$\times\left[1 + i(q l \sin\nu\cos\theta - \omega\tau)\right]$$

$$\sigma_{xz} = \sigma_{zx} = \frac{3}{2}\frac{\sigma_0}{q l\cos\nu}\sum_{n=-\infty}^{+\infty}\int_0^{\pi}\frac{d\theta\,\sin\theta\cos\theta\, J_n^2(X\cos\nu\sin\theta)}{1 + i(n\omega_c\tau - \omega\tau + q l\sin\nu\cos\theta}$$

$$\times\left[1 + i(q l\sin\nu\cos\theta - \omega\tau)\right]$$

$$\sigma_{yz} = -\sigma_{zy} = -\frac{3}{4}\frac{i\sigma_0}{\cos\nu}\sum_{n=-\infty}^{+\infty}\frac{d}{dX}\int_0^{\pi}\frac{d\theta\sin\theta\cos\theta\, J_n^2(X\cos\nu\sin\theta)}{1 + i(n\omega_c\tau - \omega\tau + q l\sin\nu\cos}$$

In the above[15], the magnetic field is in the z direction, and the y direction is perpendicular to both the magnetic field and the direction of propagation of the sound wave. The angle between the magnetic field and the direction of propagation is $\frac{\pi}{2} - \nu$. The quantity $X = \frac{q V_F}{\omega_c}$ is the sound wave number times the cyclotron radius $\left(R = \frac{V_F}{\omega_c}\right)$ and ω is the sound frequency.

In the region of geometric resonance X is of order but greater than unity, and if in addition $\left|\frac{\omega_c\tau}{1 - i\omega\tau}\right|^2 >> 1$ we need only keep the n=0 terms in the summation. The condition $X\sin\nu \leq 1$ also must be satisfied so that our results do not hold in the limit $\nu \to \frac{\pi}{2}$. However we are mainly interested in angles of tilt just beyond $\nu_c = \sin^{-1} V_s/V_F$ where V_s is the sound velocity and V_F the Fermi velocity so this condition imposes no hardship. The components of the conductivity tensor now reduce to

$$\sigma_{xx} = \frac{3\sigma_0}{(q l \cos\nu)^2}(1-i\omega\tau)\left[1 - g_0(X\cos\nu)\right]$$

$$\sigma_{yy} = \frac{3}{2}\sigma_0 \int_0^\pi \frac{\sin^3\theta\,[J_0'(X\cos\nu\sin\theta)]^2 d\theta}{1 + i(q l \sin\nu\cos\theta - \omega\tau)} \qquad \text{(II.2)}$$

$$\sigma_{zz} = \frac{3}{2}\sigma_0 \int_0^\pi \frac{d\theta\,\sin\theta\cos^2\theta\, J_0^2(X\cos\nu\sin\theta)}{1 + i(q l \sin\nu\cos\theta - \omega\tau)}$$

$$\sigma_{xy} = -\sigma_{yx} = \frac{3}{2}\frac{\sigma_0}{q l\cos\nu} g_0'(X\cos\nu) \qquad \sigma_{xz} = \sigma_{zx} = 0$$

$$\sigma_{yz} = -\sigma_{zy} = -\frac{3}{4} i \frac{\sigma_0}{\cos\nu}\frac{d}{dX}\int_0^\pi \frac{\sin\theta\cos\theta\, J_0^2(X\cos\nu\sin\theta)\,d\theta}{1 + i(q l\sin\nu\cos\theta - \omega\tau)}$$

where $g_0(X\cos\nu)$ is an oscillatory function of X previously defined.[8] We are now interested in evaluating integrals of the type that appear, e.g., in σ_{zz}. When $\omega\tau \gg 1$, the demoninator inside the integral is a rapidly varying function of θ which gives rise to a resonance when we have values of θ that satisfy $\cos\theta = \frac{V_s}{V_F}\csc\nu$ when $\sin\nu \geq V_s/V_F$. When the angle of tilt is less than the critical angle given by $\sin\nu_c = V_s/V_F$ we can no longer have a resonance effect in the denominator since the cosine cannot be greater than one. When X is not too large, the Bessel function is a slowly varying function of θ compared to the resonance denominator, and it can be taken out of the integral and evaluated at the angle $\theta^* = \cos^{-1}\frac{V_F}{V_F\sin\nu}$. The integration of the remainder of the integrand can then be easily performed to yield the following result for σ_{zz}[16]

$$\sigma_{zz} = \frac{3\sigma_0}{(q l\cos\nu)^2}(1-i\omega\tau) J_0^2(X\cos\nu\sin\theta^*)\left[N - iM\right] \qquad \text{(II.3)}$$

where N and M are functions of $\omega\tau$ and ν but not of magnetic field[12]

$$N = 1 - \frac{(G + \omega\tau H)}{2q^2} \qquad M = \frac{H - \omega\tau G}{2q^2}$$

$$G = \frac{\arctan \omega\tau\left(1 + \frac{v_F}{v_s}\sin\nu\right) - \arctan \omega\tau\left(1 - \frac{v_F}{v_s}\sin\nu\right)}{\sin\nu} \qquad \text{(II.4)}$$

$$H = \ln\left[\frac{1 + (\omega\tau)^2\left(1 + \frac{v_F}{v_s}\sin\nu\right)^2}{1 + (\omega\tau)^2\left(1 - \frac{v_F}{v_s}\sin\nu\right)^2}\right] \Big/ 2\sin\nu$$

Numerical values of the functions N and M are given in Table I for various values of $\omega\tau$ and ν .

For our further use, it proves necessary to calculate explicitly the σ_{11} component of the conductivity tensor, where we now transform to a coordinate system in which the 1 direction is the direction of propagation of the sound wave and the 2 direction is the same as the previously defined y direction. It is only necessary then to know the σ_{xx} and σ_{zz} components to compute σ_{11} . We have for σ_{11}

$$\sigma_{11} = \frac{3\sigma_0}{(q^2\cos\nu)^2}(1 - i\omega\tau)\left\{1 - g_0(X\cos\nu) + J_0^2(X\cos\nu\sin\theta^*)\left[N - iM\right]\right\} \qquad \text{(II.5)}$$

Because of the fact that we have diffusion, the effective conductivity tensor that plays an important role in ultrasonic attenuation calculations is not $\overleftrightarrow{\sigma}$ but $\overleftrightarrow{\sigma}' = \left[\overleftrightarrow{I} - \overleftrightarrow{R}\right]^{-1}\frac{\overleftrightarrow{\sigma}}{\sigma_0}$ where the tensor $\overleftrightarrow{R}$ has components[8]

$$R_{ij} = \frac{-i\omega\tau}{3\sigma_0(1 - i\omega\tau)}\left(\frac{v_F}{v_s}\right)^2 \delta_{ij}\,\sigma_{ii} \qquad \text{(II.6)}$$

The component of the effective conductivity tensor that corresponds to σ_{11} is

$$\sigma_{11}' = \frac{\frac{3\omega\tau}{(ql)^2}\left\{\left[1 - g_0 + J_0^2(N - \omega\tau M)\right] - i\omega\tau\left[1 - g_0 + J_0^2\left(N + \frac{M}{\omega\tau}\right)\right]\right\}}{(\omega\tau + J_0^2 M) + i(1 - g_0 + J_0^2 N)} \tag{II.7}$$

The approximations that were made in obtaining (II.7) are valid in the range $\nu_c \leq \nu \leq \frac{\pi}{2}$ when $\omega\tau >> 1$. The physical basis for the approximations is that orbits that are drifting along the magnetic field with a velocity that has a component in the direction of propagation equal to v_s are exactly in phase with the sound wave and therefore dominate the attenuation when $\omega\tau >> 1$. The critical angle ν_c marks the angle of tilt at which the carriers drifting along the magnetic field with the maximum velocity (i.e. v_F) are in phase with the sound wave so that only for $\nu \geq \nu_c$ can we have orbits that will be in exact phase with the sound wave.

III. Free Electron Gas

Expressions for the attenuation of sound in a free electron gas with a smeared out positive background have been derived in the literature.[8] The attenuation coefficient or power density dissipated per unit energy flux is

$$\alpha = \frac{m v_F}{M v_s} \quad \frac{S_{ii}}{I} \tag{III.1}$$

where m is the electron mass, M is the atomic mass of the metal represented by the model, l is the mean free path and S_{ii} is a diagonal component of the tensor given by

$$\overleftrightarrow{S} = Re\left\{ [\overleftrightarrow{I} + \overleftrightarrow{B}] \cdot [\overleftrightarrow{\sigma}' + \overleftrightarrow{B}]^{-1} \cdot [\overleftrightarrow{I} + \overleftrightarrow{B}] \right\} - I \qquad \text{(III.2)}$$

The tensor $\overleftrightarrow{B}$ has only diagonal components $B_{11} = -i\gamma$, $B_{22} = B_{33} = i\beta$ where $\gamma = \frac{\omega}{\omega_p^2 \tau}$ and $\beta = \gamma \left(\frac{c}{v_s}\right)^2$. Because frequencies even up to the microwave range are small compared to the plasma frequency ω_p, γ is always a small quantity. On the other hand, in the microwave range of ultrasonic frequencies β will become of order or greater than unity. Physically, for frequencies smaller than the plasma frequency the longitudinal currents must vanish because the electric fields set up by any relative charge separation will be very great. However, the electric fields set up by the relative transverse currents are weaker by a factor of $\left(\frac{v_s}{c}\right)^2$ and therefore the screening of the transverse currents breaks for microwave frequencies.

When screening breaks down $\left(\text{i.e., } |B_{ii}| > |\sigma_{ii}'| \right)$ for the transverse currents, the longitudinal component of becomes

$$S_{11} = Re \frac{1}{\sigma_{11}'} - 1 \qquad \text{(III.3)}$$

When there is no break down in screening, the expression for S_{11} contains combinations of the other components of the conductivity tensor. Detailed calculations have shown, however, that for $X > 2$ the other components of the conductivity tensor give a negligible contribution and S_{11} again

has the form (III.3). This can be seen very clearly in the case when the magnetic field and direction of propagation are perpendicular to each other from Fig. 3 in Cohen, Harrison, and Harrison.[8] In this figure, the field dependent part of S_{11} is plotted versus X for both $\beta<1$ and $\beta>1$. The curves for both cases coincide when $X>2$. Putting the expression for σ_{11}' into (III.3) we get

$$S_{11}+1 = \frac{-(q l)^2}{3[1+(\omega\tau)^2]} \left\{ \frac{J_0^2 M(\omega\tau + J_0^2 M) + [1-g_0+J_0^2 N][J_0^2 N - g_0]}{(1-g_0+J_0^2 N)^2 + J_0^4 M^2} \right\} \tag{III.4}$$

The relative attenuation $3(S_{11}+1)[1+(\omega\tau)^2]/(q l)^2$ is plotted versus $X = \frac{q v_F}{\omega_c}$ in Fig. 1. The oscillations in the attenuation are much stronger than in the case of the purely transverse field. There are maxima in where the square of the Bessel function J_0 has its maxima. Also there are minima in S_{11} where the Bessel function J_0 has its zero.[17] The values of $X \cos\nu \sin\theta^*$ where S_{11} has its maxima and minima are given in Table II.

IV. Two Spherical Band Model

A two spherical band model of a semi-metal has been studied by Harrison[14] for the calculation of ultrasonic attenuation in bismuth. In calculating the attenuation he made the assumption of equal masses and relaxation times for the holes and the electrons for the sake of simplicity. We have rederived his expressions, where necessary, without making

this assumption. We find that both the total current and the difference between the electron and hole currents respond to the sums and differences of the parameters of the two bands. The total current and the difference between the electron and hole currents are

$$\vec{J} = \vec{J}_e + \vec{J}_h = \vec{\Gamma}\cdot\left[\vec{\mathcal{E}} + \vec{q}\,\vec{q}\cdot\frac{(\vec{V}_e - \vec{V}_h)\cdot\vec{u}}{2e\iota\omega} - \left(\frac{1}{\tau_e} - \frac{1}{\tau_h}\right)\frac{m\vec{u}}{2e}\right] \tag{IV.1}$$

$$+ \vec{\Lambda}\cdot\left[\vec{q}\,\vec{q}\cdot\frac{(\vec{V}_e + \vec{V}_h)}{2e\iota\omega} - \vec{I}\left(\frac{1}{\tau_e} + \frac{1}{\tau_h}\right)\frac{m}{2e}\right]\cdot\vec{u}$$

$$\vec{J}_e - \vec{J}_h = \vec{\Gamma}\cdot\left[\vec{q}\,\vec{q}\cdot\frac{(\vec{V}_e + \vec{V}_h)}{2e\iota\omega} - \vec{I}\left(\frac{1}{\tau_e} + \frac{1}{\tau_h}\right)\frac{m}{2e}\right]\cdot\vec{u} \tag{IV.2}$$

$$+ \vec{\Lambda}\cdot\left[\vec{\mathcal{E}} + \vec{q}\,\vec{q}\cdot\frac{(\vec{V}_e - \vec{V}_h)\cdot\vec{u}}{2e\iota\omega} - \left(\frac{1}{\tau_e} - \frac{1}{\tau_h}\right)\frac{m\vec{u}}{e\tau}\right]$$

where $\vec{\Gamma} = \sigma_0^e\vec{\sigma}_e' + \sigma_0^h\vec{\sigma}_h'$ is the sum of the electron and hole conductivities and $\vec{\Lambda} = \sigma_0^e\vec{\sigma}_e' - \sigma_0^h\vec{\sigma}_h'$ is their difference. $\vec{V}_e$ and $\vec{V}_h$ are the electron and hole deformation potential tensors. In the presence of the sound wave, the energies of the electron and hole bands become, according to Harrison[17]

$$E_e = E_e^\circ - \frac{\vec{q}\cdot\vec{V}_e\cdot\vec{u}}{\omega}$$

$$E_h = E_h^\circ - \frac{\vec{q}\cdot\vec{V}_h\cdot\vec{u}}{\omega} \tag{IV.3}$$

where E_e° and E_h° are the energies of the band edges when there is no sound wave. The electric field is derivable from the currents by Maxwell's equations

$$\vec{\mathcal{E}} = \vec{F}\cdot\vec{J} \qquad \vec{F} = \begin{pmatrix} -1 & 0 & 0 \\ 0 & \epsilon\left(\frac{v_s}{c}\right)^2 & 0 \\ 0 & 0 & \epsilon\left(\frac{v_s}{c}\right)^2 \end{pmatrix}\frac{4\pi\iota}{\epsilon\omega} \tag{IV.4}$$

where ϵ is the dielectric constant of the material. The energy dissipated has been previously calculated for the two band model[14] and is

$$Q = \frac{1}{2} \mathrm{Re} \left\{ \vec{u} \cdot \left[\left\{ \frac{(\overleftrightarrow{V}_e - \overleftrightarrow{V}_n) \cdot \vec{q}\,\vec{q}}{2\epsilon\iota\omega} - \frac{m}{2e} \left(\frac{1}{\tau_a} - \frac{1}{\tau_n} \right) \overleftrightarrow{I} \right\} \cdot \vec{J} + \left\{ \frac{(\overleftrightarrow{V}_e + \overleftrightarrow{V}_n) \cdot \vec{q}\,\vec{q}}{2\epsilon\iota\omega} - \frac{m}{2e} \left(\frac{1}{\tau_a} + \frac{1}{\tau_n} \right) \overleftrightarrow{I} \right\} \cdot (\vec{j}_e - \vec{j}_n) + Nm \left(\frac{1}{\tau_e} + \frac{1}{\tau_n} \right) \cdot \vec{u} \right] \right\} \tag{IV.5}$$

Substituting (IV.1), (IV.2), and (IV.4) into (IV.5) and introducing the matrix $\overleftrightarrow{P} = \overleftrightarrow{F}^{-1}$ we find for the energy dissipated

$$Q = \frac{1}{2} \mathrm{Re} \left\{ \vec{u} \cdot \left[\frac{(\overleftrightarrow{V}_e - \overleftrightarrow{V}_n) \cdot \vec{q}\,\vec{q}}{2\epsilon\iota\omega} - \frac{m}{e} \left(\frac{1}{\tau_e} - \frac{1}{\tau_n} \right) \overleftrightarrow{I} \right] \cdot \overleftrightarrow{P} \cdot \left[\overleftrightarrow{P} - \overleftrightarrow{\Gamma} \right]^{-1} \cdot \left\{ \overleftrightarrow{\Gamma} \cdot \left[\vec{q}\,\vec{q} \cdot \frac{(\overleftrightarrow{V}_e - \overleftrightarrow{V}_n)}{2\epsilon\iota\omega} - \frac{m}{2e} \left(\frac{1}{\tau_e} - \frac{1}{\tau_n} \right) \overleftrightarrow{I} \right] + \overleftrightarrow{\Lambda} \cdot \left[\vec{q}\,\vec{q} \cdot \frac{(\overleftrightarrow{V}_e + \overleftrightarrow{V}_n)}{2\epsilon\iota\omega} - \frac{m}{2e} \left(\frac{1}{\tau_e} + \frac{1}{\tau_n} \right) \overleftrightarrow{I} \right] \right\} + \left[\frac{(\overleftrightarrow{V}_e + \overleftrightarrow{V}_n) \cdot \vec{q}\,\vec{q}}{2\epsilon\iota\omega} - \frac{m}{2e} \left(\frac{1}{\tau_e} + \frac{1}{\tau_n} \right) \overleftrightarrow{I} \right] \left\{ \overleftrightarrow{\Gamma} \cdot \left[\vec{q}\,\vec{q} \cdot \frac{(\overleftrightarrow{V}_e + \overleftrightarrow{V}_n)}{2\epsilon\iota\omega} - \frac{m}{2e} \left(\frac{1}{\tau_e} + \frac{1}{\tau_n} \right) \overleftrightarrow{I} \right] + \overleftrightarrow{\Lambda} \cdot \left[\overleftrightarrow{P} - \overleftrightarrow{\Gamma} \right]^{-1} \cdot \left[\overleftrightarrow{\Gamma} \cdot \left[\vec{q}\,\vec{q} \cdot \frac{(\overleftrightarrow{V}_e - \overleftrightarrow{V}_n)}{2\epsilon\iota\omega} - \frac{m}{2e} \left(\frac{1}{\tau_e} - \frac{1}{\tau_n} \right) \overleftrightarrow{I} \right] + \overleftrightarrow{\Lambda} \cdot \left[\vec{q}\,\vec{q} \cdot \frac{(\overleftrightarrow{V}_e + \overleftrightarrow{V}_n)}{2\epsilon\iota\omega} - \frac{m}{2e} \left(\frac{1}{\tau_e} + \frac{1}{\tau_n} \right) \overleftrightarrow{I} \right] \right] \right\} + Nm \left(\frac{1}{\tau_e} + \frac{1}{\tau_n} \right) \overleftrightarrow{I} \cdot \vec{u} \right\} \tag{IV.6}$$

In the case where the deformation forces are strong i.e.

$$\left| \frac{q\,|\,V_{ii}}{2mv_F^2} \; \frac{v_F}{v_s} \right| >> 1$$

, we obtain for Q

$$Q = N m |\vec{u}|^2 \left(\frac{1}{\tau_e} + \frac{1}{\tau_n}\right) \hat{u} \cdot \overleftrightarrow{S} \cdot \hat{u} \qquad \text{(IV.7)}$$

where

$$\overleftrightarrow{S} = \overleftrightarrow{I} + \frac{\tau_e \tau_n}{N e^2 m \omega^2 (\tau_e + \tau_n)} Re \Big\{ (\vec{V}_e - \vec{V}_n) \cdot \vec{q}\,\vec{q} \cdot \overleftrightarrow{P} \cdot [\overleftrightarrow{P} - \overleftrightarrow{\Gamma}]^{-1} \cdot \overleftrightarrow{\Gamma} \cdot \vec{q}\,\vec{q} \cdot (\vec{V}_e - \vec{V}_n) + (\vec{V}_e + \vec{V}_n) \cdot \vec{q}\,\vec{q} \cdot \Big\{ \overleftrightarrow{\Gamma} + \overleftrightarrow{\Lambda} \cdot [\overleftrightarrow{P} - \overleftrightarrow{\Gamma}]^{-1} \cdot \overleftrightarrow{\Lambda} \Big\} \cdot \vec{q}\,\vec{q} \cdot (\vec{V}_e + \vec{V}_n) + (\vec{V}_e - \vec{V}_h) \cdot \vec{q}\,\vec{q} \cdot \Big\{ \overleftrightarrow{\Lambda} + \overleftrightarrow{P} \cdot [\overleftrightarrow{P} - \overleftrightarrow{\Gamma}]^{-1} \cdot \overleftrightarrow{\Lambda} + \overleftrightarrow{\Lambda} \cdot [\overleftrightarrow{P} - \overleftrightarrow{\Gamma}]^{-1} \cdot \overleftrightarrow{\Gamma} \Big\} \cdot \vec{q}\,\vec{q} \cdot (\vec{V}_e + \vec{V}_h) \Big\} \qquad \text{(IV.7')}$$

The restriction to strong deformation forces is easily satisfied in the semi-metals where it has been estimated[14] that the quantity above is $\sim 10^3$. For the attenuation of a longitudinally polarized sound wave we get

$$S_{11} = 1 + \frac{\tau_e \tau_n}{4 N e^2 (\tau_e + \tau_n)} \frac{q^2}{\rho V_s^2} Re \Big\{ (V_{De} + V_{Dh})^2 \Big[\Gamma_{11} + \Lambda_{1i} [\overleftrightarrow{P} - \overleftrightarrow{\Gamma}]^{-1}_{ij} \Lambda_{j1} \Big] + (V_{De} - V_{Dh})^2 P_{11} [\overleftrightarrow{P} - \overleftrightarrow{\Gamma}]^{-1}_{1i} \Gamma_{i1} + (V_{De}^2 - V_{Dh}^2) \Big[\Lambda_{11} + P_{11} [\overleftrightarrow{P} - \overleftrightarrow{\Gamma}]^{-1}_{1i} \Lambda_{i1} + \Lambda_{1i} [\overleftrightarrow{P} - \overleftrightarrow{\Gamma}]^{-1}_{ij} \Gamma_{j1} \Big\} \qquad \text{(IV.8)}$$

All the terms in above expression which contain P_{11} can be neglected when we are at sound frequencies below the plasma frequency; then we have screening, and the longitudinal currents nearly vanish. Therefore as long as the electron and hole deformation potentials are not nearly 180° out of

phase (i.e., $V_{0e} \neq -V_{0h}$), only the terms containing the sum of the deformation potentials remain. The second term in the expression containing the sum of the deformation potentials has been calculated explicitly and has been found to be negligible except in the region of Harrison's high field peak for frequencies of interest (i.e. in the frequency region > 10 mc for Bi). Therefore, in the regions of geometric resonance and also in the region of the high field tilt effect we have

$$S_{11} = 1 + \frac{\tau_e \tau_h}{4Ne^2 m(\tau_e + \tau_h)} \frac{q^2}{V_s^2} (V_{0e} + V_{0h})^2 \, Re \, \Gamma_{11} \tag{IV.9}$$

and we can see that the contributions to the ultrasonic absorption from the two bands are additive. Because of this additivity, the contributions of each of the bands to geometric resonance and to the tilt effect are separable. The assumptions of equal effective masses and relaxation times for the two bands are therefore not unduly restrictive in interpreting results from experimental data.

We now return to the assumptions of equal masses and relaxation times to calculate S_{11} for the case of geometric resonance in tilted magnetic fields. As we have just shown, for values of the deformation potential and the frequency ranges of interest, these assumptions are not restrictive. We then have

$$(S_{11} - 1) \Big/ \frac{m}{m^*} \left(\frac{V_{0e} + V_{0h}}{2mv_F^2} \right)^2 \left(\frac{v_F}{v_s} \right)^2 (ql)^2 = Re \, \sigma_{11}' \tag{IV.10}$$

where m^* is the effective mass of the carriers and m is the free electron mass. Substituting the expression obtained for σ_{11}' (II.7) into (IV.10), we obtain for the normalized attenuation

$$(S_{11}-1)\Big/\frac{m}{m^*}\left(\frac{V_{oe}+V_{oh}}{2mv_F^2}\right)^2(ql)^2 = \frac{-3\left\{J_o^2M(\omega\tau+J_o^2M)+\left[1-g_o+J_o^2N\right]\left[NJ_o^2-g_o\right]\right\}}{\left[\omega\tau+J_o^2M\right]^2+\left[1-g_o+J_o^2N\right]^2}$$

(IV.11)

The normalized attenuation is plotted versus X in Fig. 2. The oscillations of the attenuation with X are very similar to those shown in Fig. 1 for the model of a free electron gas. The only difference between the two figures besides a difference in scale occurs in the high field limit. Therefore we can expect very similar results for both models in the geometric resonance region except for the orders of magnitude of the effect.

V. Majority and Minority Carriers

We now calculate the ultrasonic attenuation for a model of majority and minority carriers with a positive background to represent the positively charged ions. The model is appropriate when we have a small section of the Fermi surface which has a much smaller Fermi velocity than the remainder of the Fermi surface. We assume that we have two spherical pieces of Fermi surface with Fermi velocities V_{F1} and V_{F2} and numbers of carriers n_1 and n_2 ($n_i = \frac{1}{3\pi^2}\left(\frac{mV_{Fi}}{\hbar}\right)^3$) such that $n_1+n_2 = n_o$, where n_o is the number of positive ions smeared out in the background.

To make the calculation simpler we assume that the effective masses and relaxation times of the two kinds of carriers are equal.

The total current contains a contribution from the positive background as well as from the two types of carriers

$$\vec{J} = \vec{J}_{e1} + \vec{J}_{e2} + n_0 e \vec{u} \tag{V.1}$$

The electromagnetic field set up by the passage of the sound wave can be calculated self-consistently from Maxwell's equations. We can write the relation between the electric field and the total current as

$$\vec{J} = -\sigma_0 \vec{\vec{B}} \cdot \vec{\mathcal{E}} \tag{V.2}$$

where $\vec{\vec{B}}$ is the diagonal matrix defined in Section III with components $B_{11} = -\iota\gamma$, $B_{22} = B_{33} = \iota\beta$ and $\sigma_0 = \frac{n_0 e^2 \tau}{m}$. From the solution of Boltzmann's equations and (V.1) we obtain

$$\vec{J}_{e1} = \sigma_{01} \vec{\vec{\sigma}}_1' \left(\vec{\mathcal{E}} - \frac{m\vec{u}}{e\tau}\right) \qquad \vec{J}_{e2} = \sigma_{02} \vec{\vec{\sigma}}_2' \left(\vec{\mathcal{E}} - \frac{m\vec{u}}{e\tau}\right)$$

$$\sigma_{01} = \frac{n_1 e^2 \tau}{m} \qquad \sigma_{02} = \frac{n_2 e^2 \tau}{m} \tag{V.3}$$

where $\vec{\vec{\sigma}}_1'$ and $\vec{\vec{\sigma}}_2'$ are the effective conductivity tensors for the two kinds of carriers. The energy dissipated per unit volume in the case of the majority and minority carriers is

$$Q = \frac{1}{2} Re \left\{ (\vec{J}_{e1}^{*} + \vec{J}_{e2}^{*}) \cdot \vec{\mathcal{E}} - \vec{u}^{*} \frac{n_1 m}{\tau} (\langle \vec{v}_{e1} \rangle - \vec{u}) - \vec{u}^{*} \frac{n_2 m}{\tau} (\langle \vec{v}_{e2} \rangle - \vec{u}) \right\} \tag{V.4}$$

where the first term inside the brackets is the energy transferred from the sound wave to the two types of carriers and the last two terms are the energy fed back into the sound wave because of the drag exerted by the two kinds of carriers on the positive background. These drag forces arise because the average carrier velocity $\langle \vec{v}_{ei} \rangle$ before collision in general differs from that after collision.[18] Using (V.1) and (V.2) to simplify (V.4) we have

$$Q = -\frac{1}{2} Re \left\{ n_0 e \vec{u}^{*} \cdot (\overleftrightarrow{I} + \overleftrightarrow{B}) \cdot \vec{\mathcal{E}} \right\} \tag{V.5}$$

We can now use (V.1), (V.2) and (V.3) to obtain the electric field in terms of the sound field $\vec{u}$ set up by the sound wave

$$\vec{\mathcal{E}} = -\left[\overleftrightarrow{B} + \frac{n_1}{n_0} \overleftrightarrow{\sigma}_1' + \frac{n_2}{n_0} \overleftrightarrow{\sigma}_2' \right]^{-1} \cdot \left[\overleftrightarrow{I} - \frac{n_1}{n_0} \overleftrightarrow{\sigma}_1' - \frac{n_2}{n_0} \overleftrightarrow{\sigma}_2' \right] \cdot \frac{m \vec{u}}{e \tau} \tag{V.6}$$

We can see that the conductivity tensors of the two types of carriers come in only in the form $\frac{n_1}{n_0} \overleftrightarrow{\sigma}_1' + \frac{n_2}{n_0} \overleftrightarrow{\sigma}_2'$. In other words, their contribution comes in the form of the effective conductivity tensor of a

group of carriers weighted by the fraction of the total number of carriers in the group. Thus for the tensor $\overleftrightarrow{S}$ which is directly related to the absorption we have

$$\overleftrightarrow{S} = Re\left\{ \left[\overleftrightarrow{I} + \overleftrightarrow{B}\right] \cdot \left[\overleftrightarrow{B} + \frac{n_1}{n_0}\overleftrightarrow{\sigma_1}' + \frac{n_2}{n_0}\overleftrightarrow{\sigma_2}'\right]^{-1} \cdot \left[\overleftrightarrow{I} + \overleftrightarrow{B}\right] \right\} - 1 \qquad (V.7)$$

For the ratio of the Fermi velocities of the minority to the majority carriers we have assumed $v_{F1}/v_{F2} \simeq 0.1$. Therefore we have $\frac{n_1}{n_0} \simeq 10^{-3}$ and $\frac{n_2}{n_0} \simeq 1$. If the minority carriers are in the region of geometric resonance, i.e. $X_1 = \frac{q v_F}{\omega_c} \geq 1$, then the majority carriers are in the region between geometric resonance and cyclotron resonance, i.e. $X_2 \geq 10$, and their conductivity tensor is not strongly dependent on magnetic field.

To calculate the attenuation of longitudinally polarized waves when either $\beta > 1$ or $\beta < 1$ and $X_1 > 2$ we can use (III.3) by replacing σ_{11}' by $\frac{n_1}{n_0}\sigma_{11}^{1\prime} + \frac{n_2}{n_0}\sigma_{11}^{2\prime}$. For the majority carriers we get $\sigma_{11}^{2\prime} = \frac{3\iota\omega\tau}{(q l_2)^2}$ by using the limiting form of the expressions (II.1) for large X .

We first treat the case where the magnetic field is transverse to the direction of propagation. The conductivity tensor for the minority carriers is

$$\sigma_{11}^{1\prime} = -\frac{3\iota\omega\tau}{(q l_1)^2} \frac{(1-\iota\omega\tau)\left[1 - g_0(X_1)\right]}{\left[1 - \iota\omega\tau - g_0(X_1)\right]} \qquad (V.8)$$

Using these expressions for the conductivity tensors of the minority and majority carriers, we get for the attenuation when the minority carriers

are in the region of geometric resonance

$$S_{11}+1 = \frac{\frac{V_{F2}}{3V_{F1}}(ql_1)^2 g_0(X_1)\left[1-g_0(X_1)\right]}{\left(1+\frac{V_{F1}}{V_{F2}}\right)^2\left\{\left[1-g_0(X_1)\right]^2+(\omega\tau)^2\left[1-\frac{g_0(X_1)\frac{V_{F1}}{V_{F2}}}{1+\frac{V_{F1}}{V_{F2}}}\right]^2\right\}} \quad (V.9)$$

From (V.9) we can see that a small number of carriers in the geometric resonance region dominates the attenuation despite the presence of a large number of carriers which do not satisfy the geometric resonance criterion. The expression (V.9) resembles the expression for the attenuation of longitudinal waves in a free electron gas model[8] except for the factor $\frac{V_{F2}}{V_{F1}}$ which arises from the difference in the Fermi velocities of the two kinds of carriers. Therefore if we have small sections of the Fermi surface on geometric resonance, we will be able to observe the oscillations due to these sections although the remainder of the Fermi surface is not in the geometric resonance region. We can now proceed to the calculation of the attenuation for geometric resonances in tilted magnetic fields. The conductivity component for the majority carriers is again $\sigma_{11}^{2'} \simeq -\frac{3i\omega\tau}{(ql_2)^2}$. We can use (II.7) for the appropriate component of the conductivity tensor for the minority carriers. The attenuation then becomes

$$S_{11}+1 = \frac{-\frac{V_{F2}}{3V_{F1}}(ql_1)^2\left[J_0^2M(\omega\tau+J_0^2M)+(1-g_0+J_0^2N)(J_0^2N-g_0)\right]}{\left[1+\frac{V_{F1}}{V_{F2}}\right]^2\left\{\left[1-g_0+J_0^2\left(N-\omega\tau\frac{V_{F1}}{V_{F2}}M\right)\right]^2+(\omega\tau)^2\right\}} \quad (V.10)$$

where we have dropped terms that are of order $\left(\frac{1}{\omega\tau}\right)^2$. The part of the attenuation that depends upon the magnetic field and the angle of tilt is similar to that of the two band model developed in Section IV. Therefore we have the same general type of geometric resonance in tilted magnetic fields as in the case of a semi-metal except for a scale factor. In the case of majority and minority carriers in tilted fields, the minority carriers dominate the attenuation as in the case of the non-tilted field discussed earlier in this section. Therefore we can use geometric resonances in tilted fields the map out small sections of the Fermi surfaces as in the two cases discussed previously despite the presence of the remainder of the Fermi surface. This is important because, for many materials, only small portions of the Fermi surface have a Fermi velocity small enough for the tilt effect to occur at measurably large angles.

VII. Discussion

In our calculations in Sections III, IV, and V we have found geometric resonances in tilted magnetic fields, the form of which, apart from field and angular independent scale factors, seems to be independent of the model used for the calculation. The only qualitative difference between the models used appears in the high field limit. Moreover, the oscillations which appear in the case of tilted fields are much stronger than those which appear in transverse fields. Mathematically, in the tilted field case the oscillations arise from the Bessel functions $J_0(X \cos\psi \sin\theta^*)$ which have zeros at certain values of X . In the case of exactly transverse field the oscillations arose from the

less rapidly varying $g_0(X)$ which does not have any zeroes and which is the square of the Bessel function averaged over the whole Fermi surface. Physically, in the tilted field case, we have one orbit dominating the attenuation instead of an average over all orbits which gives a heavy weight to extremal orbits and which nearly washes out the amplitude of the oscillations.

When the magnetic field is tilted from the direction perpendicular to the direction of propagation, there are no orbits drifting along the magnetic field in exact phase with the sound wave until we reach the critical angle ν_c, given by $\sin \nu_c = \frac{v_s}{v_F}$. At this angle, carriers drifting along the magnetic field, which are at the tip of the Fermi surface, have a component of drift velocity in the direction of propagation equal to the velocity of sound. These carriers therefore drift in exact phase with the sound wave, and they dominate the attenuation. As we increase the angle of tilt beyond the critical angle, other orbits drift in phase with the sound wave, and they dominate the attenuation. By varying the angle of tilt, we can therefore bring orbits from all over the Fermi surface into phase with the sound wave and make them dominate the attenuation. We can then, by varying the strength of the magnetic field, get geometric resonances from each orbit that dominates the attenuation separately.

The condition for a maximum in the oscillations when the magnetic field is tilted at an angle ν is

$$d \cos \nu \cong n\lambda \tag{VI.1}$$

where $d = \frac{c p_F}{e H} \sin \theta^*$ is the cyclotron diameter in real space and

$p_F \sin\theta^*$ is the dimension of the Fermi surface transverse to both the magnetic field and the direction of propagation. The situation is shown in Fig. 3. It is the projection of the cyclotron diameter in real space in the direction of propagation that must be equal to an integral number of wave lengths. The drift velocity of the orbit along the magnetic field can also be obtained since the component of the drift velocity along the direction of propagation must be equal to the velocity of sound for the orbit to dominate the attenuation. Therefore at an angle of tilt ν, the orbit dominating the attenuation has a drift velocity of

$$v_H = \frac{v_s}{\sin\nu} \qquad \text{(VI.2)}$$

The relationship between the angle of tilt and the drift velocity is shown in Fig. 4. Therefore the linear dimensions of the Fermi surface and the drift velocities can be determined everywhere if $\omega\tau >> 1$ and the angle of tilt occurs at measurably large angles.

The condition $\omega\tau >> 1$ arises because for an orbit to dominate the absorption, it must drift in phase with the sound wave for many periods before the carriers traversing the orbit are scattered to other orbits. If this condition is not well satisfied, then we obtain comparable or greater contributions from orbits other than the one we are interested in and we are no longer able to determine the dimensions and drift velocity of a single orbit. The requirement that the angle of tilt occur at measurably large angles arises because the solid angle of the Fermi surface mapped out is a very rapid function of angle of tilt, for

angles just beyond ν_c . Therefore if this requirement is not satisfied, only a small solid angle of the Fermi surface around its extremal dimensions would be mapped out and no new information would be gained.

The condition $\omega\tau >> 1$ would require microwave sound waves and materials of ultra-high purities except perhaps for the semi-metals and tin, zinc, and c 'um among others. The requirement that the angle of tilt occur at mea bly large angles is satisfied if there are sections of the Fermi surfa ith a small Fermi velocity such as occurs in the semi-metals and in certain portions of the Fermi surfaces of tin, zinc, magnesium, gallium, etc.

In materials where the conditions for observing the combined geometric resonance-tilt effect phenomena are satisfied, it should prove a very important tool in determining the electronic band structure. In materials in which the condition $\omega\tau >> 1$ is only marginally satisfied, we can still identify the first few oscillations with the orbit drifting in exact phase with the sound wave, as the discussion in Appendices A and B shows. The remaining oscillations would be harder to interpret experimentally, as in the region beyond the first few oscillations, orbits other than the one drifting in phase contribute significantly to the attenuation.

We note, in passing, that the strong oscillations observed by Morse in the noble metals for the dog's bone[11] orbit[19] are more reminiscent of the geometric resonances occurring in tilted fields than of those predicted by Cohen, Harrison, and Harrison in the free electron model for transverse field. In the case of the "dog's bone orbits, all the orbits contributing to the attenuation have very nearly the same diameter in

momentum space. Therefore we would have, as in the case of tilted fields, one orbit or type of orbit dominating the attenuation instead of an average over all the orbits. These would result in the oscillations being much stronger than predicted by the free electron model. We have already shown in Section V that those orbits on the Fermi surface that are in the geometric resonance region will dominate the attenuation even in the case of transverse magnetic fields.

Acknowledgment

The author is very grateful to Professor M. H. Cohen for his continued encouragement in many valuable discussions and for first calling his attention to the interesting phenomena discussed in this paper.

Appendix A

The evaluation of the rapidly varying part of the integrand discussed in Section II and the validity of the approximations made in treating it as rapidly varying compared to the Bessel function warrant further discussion. The remainder of the integrand, after the slowly varying part has been removed, is of the form

$$\int_{-1}^{1} \frac{dx}{1 + i\omega\tau\left(\frac{V_F}{V_S}\sin\nu x - 1\right)} \tag{A.1}$$

For large $\omega\tau$, there is a relation[21] that enables us to replace the integrand by

$$\lim_{\omega\tau\to\infty} \frac{1}{\frac{V_F}{V_S}\sin\nu x - 1 - \frac{i}{\omega\tau}} = \frac{P}{\frac{V_F}{V_S}\sin\nu x - 1} + i\pi\,\delta\left(\frac{V_F}{V_S}\sin\nu x - 1\right) \tag{A.2}$$

where P stands for the principal part of the function. Therefore when $\omega\tau >> 1$, the approximation made in treating the denominator of the integrals appearing in (II.2) as rapidly varying is more readily justifiable for the real part of the integral (A.1) than it is for the imaginary part. For a better approximation with $\omega\tau$ not too large, we can evaluate the rapidly varying integral (A.1) directly. The real and imaginary parts of (A.1) are the functions G and H defined in (II.4). The functions G and H are given for various values of $\omega\tau$ and ν in Table III.

It may also be noted that the approximations made in deriving (II.3)

are least valid where the Bessel function $J_0(X\cos\nu\sin\theta)$ has its zeroes. To evaluate the approximations made, in this region, we expand $J_0^2(X\cos\nu\sin\theta)$ around the angle θ^*

$$J_0^2(X\cos\nu\sin\theta) = J_0^2(X\cos\nu\sin\theta^*) + X\cos\nu(\sin\theta-\sin\theta^*)\frac{d}{d(X\cos\nu\sin\theta^*)}J_0^2(X\cos\nu\sin\theta^*) + \frac{1}{2}X^2\cos^2\nu(\sin\theta-\sin\theta^*)^2 \times \frac{d^2J_0^2(X\cos\nu\sin\theta^*)}{d(X\cos\nu\sin\theta^*)^2} \tag{A.3}$$

The square of the Bessel function is an even function of $\sin\theta$ so that when $J_0^2(X\cos\nu\sin\theta^*) = 0$ we have

$$J_0^2(X\cos\nu\sin\theta) = \frac{1}{2}X^2\cos^2\nu(\sin\theta-\sin\theta^*)^2 J_1^2(X\cos\nu\sin\theta^*) \tag{A.4}$$

where we have used the familiar Bessel function identities[22] $2J_\nu' = J_{\nu-1} - J_\nu$ and $J_{-\nu} = (-1)^\nu J_\nu$. Substituting the expansion (A.3) for $J_0^2(X\cos\nu\sin\theta)$ in the integral in (II.2) we get an expansion in terms of the derivatives of $J_0^2(X\cos\nu\sin\theta)$ evaluated at θ^*. The coefficient of the n^{th} derivative in this expansion has been calculated to be of order $\left(\frac{\cot\nu}{\omega_c\tau}\right)^n$. Therefore the condition for the approximations made in deriving (II.3) to be valid is that $\cot\nu < \omega_c\tau$. We can rewrite this condition in terms of the parameters q_1 and X

$$X\cot\nu < q_1 \tag{A.5}$$

This condition arises because for values of X which violate this condition the Bessel function is not a slowly varying function of θ compared to the denominator of the integral and the approximation breaks down. For $\omega\tau = 10$ and $\nu = 0.01$, the condition for the validity of the approximation is that $X < 10$ so that only the first few oscillations can be easily interpreted as coming from a given orbit. We can see from (A.5) that we can increase the value of X for which the approximations made are valid by increasing q.

Appendix B

In Appendix A we noted that when $J_0(X \cos\nu \sin\theta')$ has its zeroes, the approximations used in deriving were not valid and that we must use expression (A.3) instead. Introducing (A.4) into the expression for in (II.3) we find that

$$\sigma_{11}' = \frac{3\omega\tau}{(q1)^2} \left\{ \left[1 - g_0 + \frac{1}{2} \frac{\cot^2\nu}{(\omega_c\tau)^2} J_1^2 (N - \omega\tau M) - i\omega\tau \left[1 - g_0 + \frac{1}{2} \frac{\cot^2\nu}{(\omega_c\tau)^2} J_1^2 \left(N + \frac{M}{\omega\tau}\right)\right]\right] \right. \tag{B.1}$$

$$\left. \frac{}{\left[\omega\tau + \frac{1}{2} \frac{\cot^2\nu}{(\omega_c\tau)^2} J_1^2 M\right] + i \left[1 - g_0 + \frac{1}{2} \frac{\cot^2\nu}{(\omega_c\tau)^2} J_1^2 N \right]} \right.$$

Account has been taken of the correction to (II.7) contained in (B.1), when the Bessel function J_0 has its zeroes, in calculating the relative attenuation shown in Figures 1 and 2. The effect of the correction is to decrease the peak to valley ratio from what it would be from (III.4) and (IV.11) without considering the correction.

References

1. R. W. Morse and J. D. Gavenda, Phys. Rev. Lett. 2, 250 (1959).
2. R. W. Morse, A. Myers, and C. T. Walker, Phys. Rev. Lett. 4, 605 (1960).
3. H. E. Bommel, Phys. Rev. 100, 758 (1955); W. P. Mason and H. E. Bommel, J. Acoust. Soc. Amer. 28, 930 (1956).
4. T. Olsen, Phys. Rev. 118, 1007 (1960).
5. B. W. Roberts, Phys. Rev. 119, 1889 (1960).
6. A. A. Galkin and A. P. Korolyuj, K. Exptl. Theoret. Phys. (U.S.S.R.) 38, 1688 (1960) [translation: Soviet Phys. JETP 11, 1218 (1960)].
7. D. H. Reneker, Phys. Rev. 115, 303 (1959).
8. M. H. Cohen, M. J. Harrison, and W. A. Harrison, Phys. Rev. 117, 937 (1960).
9. T. Kjeldaas and T. Holstein, Phys. Rev. Lett. 2, 340 (1959).
10. A. B. Pippard, Proc. Roy. Soc. A 257, 165 (1960).
11. V. L. Gurevich, J Exptl. Theoret. Phys. (U.S.S.R.) 37, 71 (1959) [translation: Soviet Phys. JETP 10, 51 (1960)].
12. H. N. Spector, Phys. Rev. 120, 1261 (1960).
13. H. N. Spector (to be published in Phys. Rev. Lett.).
14. M. J. Harrison, Phys. Rev. 119, 1260 (1960).
15. It is to be noted that the sign of the carriers, i.e. whether they are electrons or holes, comes into the expressions for the conductivity tensor through the quantity X. Therefore the symmetric components of the conductivity tensor, i.e. σ_{xx}, σ_{yy}, σ_{zz} and σ_{xz}, are the same for both the electrons and the holes while the anti-symmetric components, i.e. σ_{xy} and σ_{yz} change sign for electrons and holes.

16. Further discussion of the mathematical approximations used to derive (II.3) and their range of validity is given in Appendix A.

17. Further discussion of the behavior of S_{11} at the values of $X \cos\nu \sin\theta^*$ near where J_0 has its zeroes is given in Appendix B.

18. M. J. Harrison (Private Communication).

19. T. Holstein, Phys. Rev. 113, 479 (1959).

20. R. W. Morse, in "The Fermi Surface", edited by W. A. Harrison and M. B. Webb (John Wiley and Sons, Inc., New York, 1960), pp. 214-23.

21. P. M. Morse and H. Feshbach, "Methods of Theoretical Physics", Vol. I (McGraw Hill, 1953), p. 473.

22. Reference 21, Vol. II, p. 1322.

Figure Captions

Fig. 1 -- The normalized attenuation $3(S_{11}+1)[1+(\omega\tau)^2]/(q\ell)^2$ is plotted versus $X = qR$ for the model of a free electron gas. The angle of tilt in this case is $\nu = 0.02$ and $\omega\tau = 10$ The plot is correct for all magnetic fields when the screening of the transverse currents breaks down and is correct for $qR > 2$ when screening does not break down. In the region shown, the oscillations can be attributed to a single orbit.

Fig. 2 -- The normalized attenuation $(S_{11}-1)/\frac{m}{m^*}\left(\frac{V_{0e}+V_{0h}}{2mv_F^2}\right)^2(q\ell)^2$ as a function of $X = qR$ for a two spherical band model consisting of electrons and holes. The plot is for an angle of tilt of $\nu = 0.02$ and $\omega\tau = 10$. The normalized attenuation $q(S_{11}+1)/(q\ell_1)^2\left(\frac{v_{F2}}{v_{F1}}\right)$ for the case of minority and majority carriers when the ratio $\frac{v_{F2}}{v_{F1}} = 10$ follows the same plot for the same values of ν and $\omega\tau$. The oscillations in the region shown can be attributed to the orbit drifting in phase with the sound wave.

Fig. 3 -- When the magnetic field is tilted at an angle ν in the direction of the sound wave, the orbit gives rise to a maximum in the attenuation when the component of the orbit diameter in the direction of propagation is equal to an integral number of wavelengths.

Fig. 4 -- The orbit which dominates the attenuation is shown to drift along the magnetic field with a velocity $v_s/v_H \sin\nu$.

Table I

Values of the functions N and M for $\omega\tau$ = 1, 10 and 100 and angles of tilt from ν = 0.008 to 0.015

	$\omega\tau$ = 10		$\omega\tau$ = 100	
ν	N	M	N	M
0.007	-0.221	-0.065	-0.239	-0.007
0.008	-0.331	-0.126	-0.373	-0.014
0.009	-0.484	-0.261	-0.634	-0.036
0.010	-0.574	-0.610	-1.657	-0.756
0.011	-0.232	-0.928	-0.395	-1.367
0.012	-0.062	-0.999	-0.011	-1.276
0.013	+0.13	-0.994	0.205	-1.186
0.014	0.268	-0.957	0.349	-1.105
0.015	0.373	-0.912	0.453	-1.034

	$\omega\tau$ = 1	
ν	N	M
0.007	0.017	-0.073
0.008	0.018	-0.104
0.009	0.028	-0.128
0.010	0.043	-0.153
0.011	0.060	-0.178
0.012	0.078	-0.203
0.013	0.105	-0.220
0.014	0.129	-0.243
0.015	0.151	-0.257

Table II

Magnitude of $d\cos\nu = \chi \sin\theta^* \cos\nu$ at Extrema of S_{ij}

Maxima		Minima
0	(1.29)*	2.41
3.84		5.52
7.02		8.65

*For the free electron case, the first maxima occurs at this value; all the other extrema occur at the same values of $d\cos\nu$ for the various models considered.

Table III

Values of the function G and H for $\omega\tau$ = 1, 10, and 100 and angles of tilt from ν = 0.007 to 0.015.

	$\omega\tau$ = 1		$\omega\tau$ = 10		$\omega\tau$ = 100	
ν	G	H	G	H	G	H
0.007	105.7	90.9	37.1	240.5	3.92	247.8
0.008	108.7	87.9	51.2	261	5.55	274.5
0.009	110	84.3	81.1	288.8	10.49	326.7
0.010	111	80.5	152	299.6	156.6	529.8
0.011	111.8	76.3	210	245.4	276.1	276.3
0.012	112.5	71.9	219	190.6	257.3	199.7
0.013	111.5	67.4	214	152.7	238.8	156.7
0.014	111.4	62.8	204	125.9	222.3	127.9
0.015	110	58.6	193	106	207.8	107.3

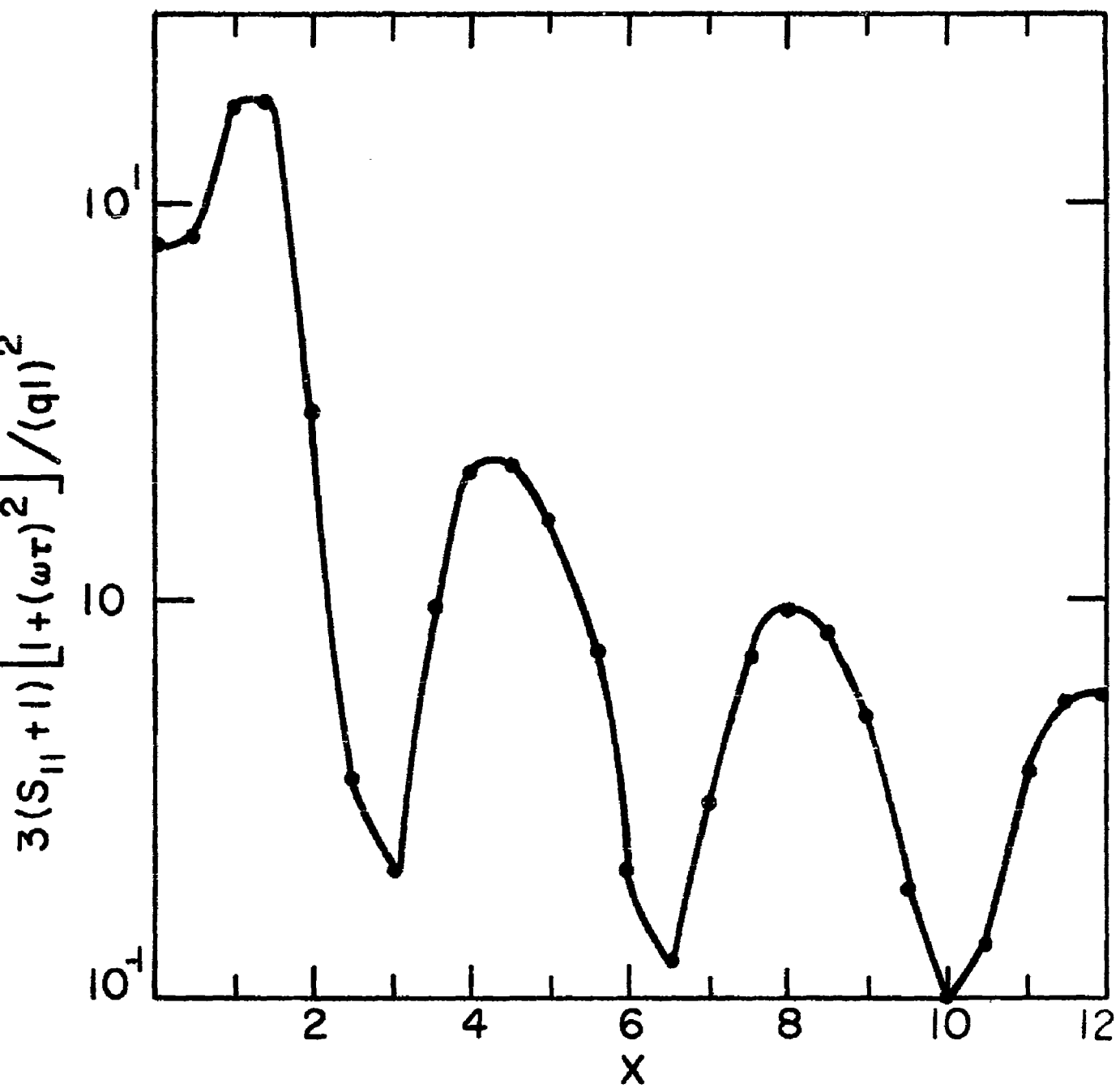

Fig.1

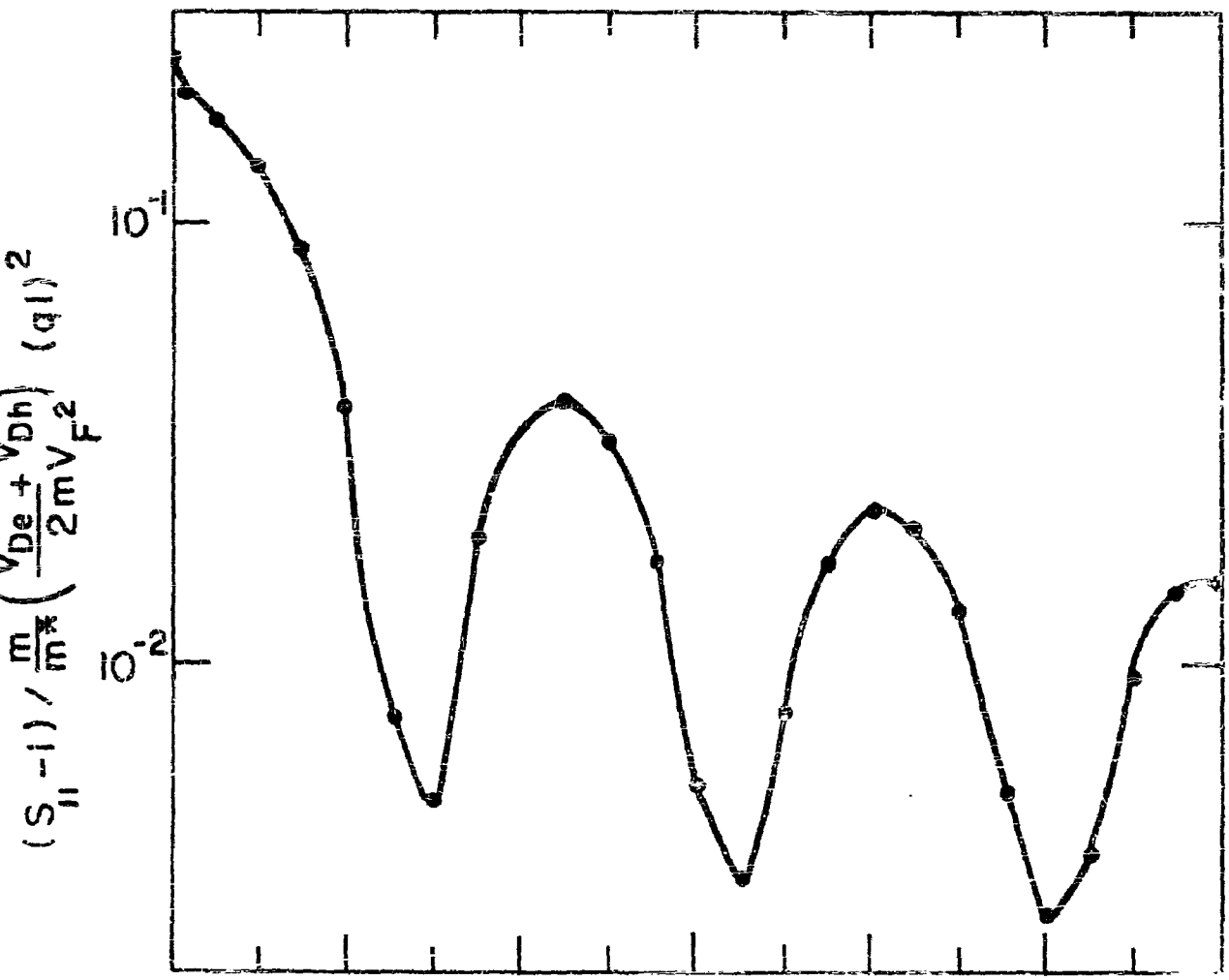
$(S_{11}-1) / \frac{m}{m^*}\left(\frac{V_{De}+V_{Dh}}{2mV_F^2}\right)^2 (ql)^2$
10^{-1}
10^{-2}
2
4
6
8
10
12
X

Fig. 2

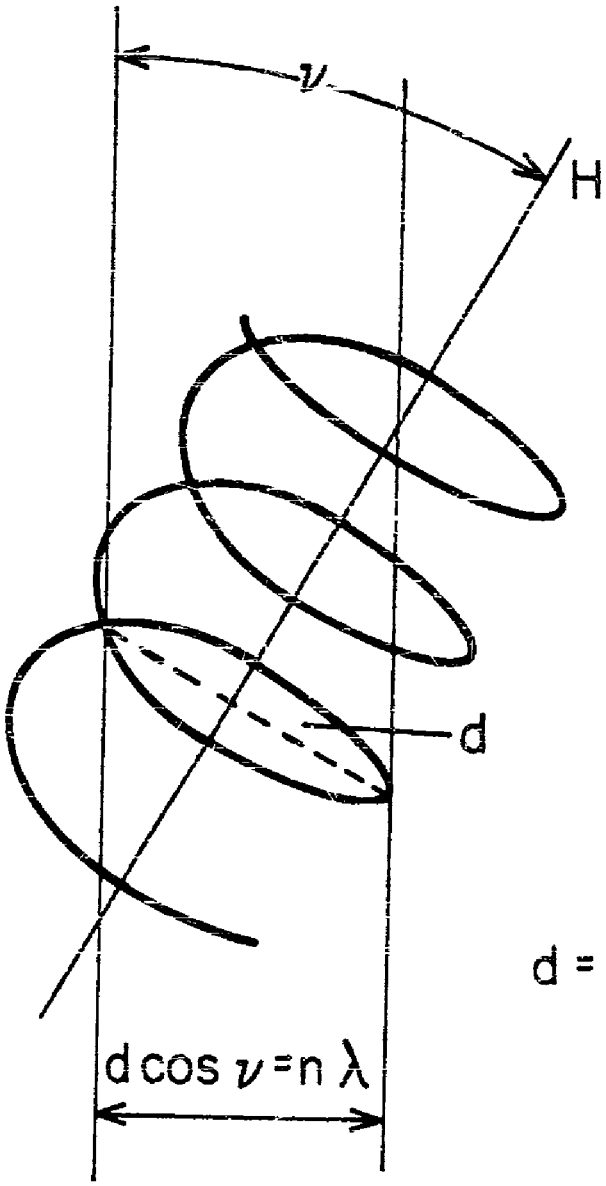

$$d = \frac{e\, p_F \sin\theta}{c\, H}$$

Fig. 3

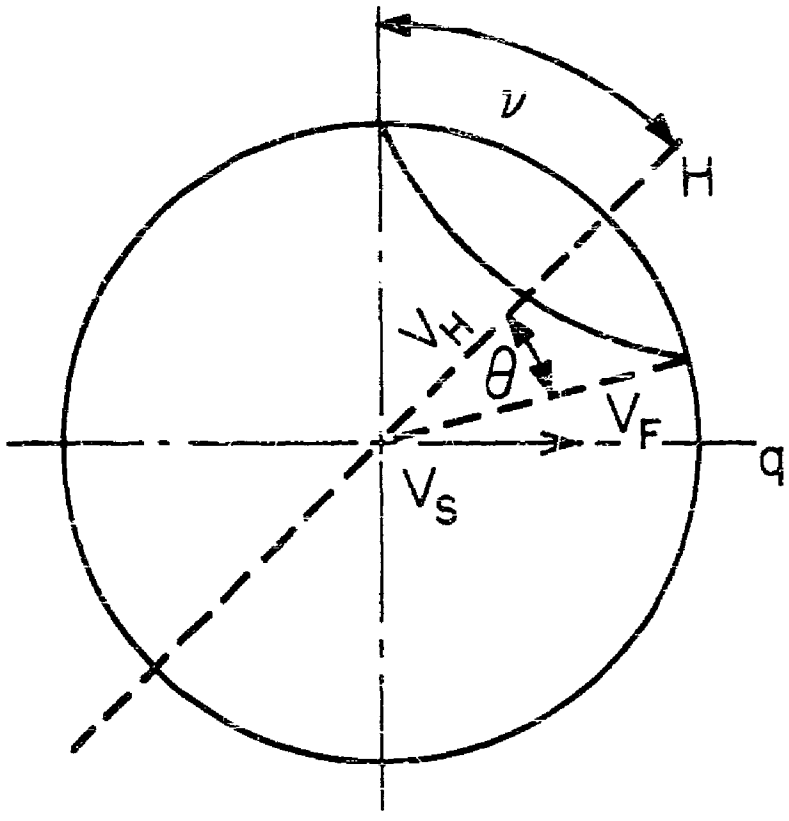

$$V_H = V_F \cos. \theta$$

$$V_H \sin. \nu = V_S$$

Fig. 4

UNCLASSIFIED